

# 3D Imaging of Optically Cleared Spheroids in Corning® Spheroid Microplates

## Application Note

CORNING

Thomas S. Villani<sup>1</sup>, Graeme Gradner<sup>1</sup>, Michael T. Johnson<sup>1</sup>,  
Hilary Sherman<sup>2</sup>, and Ann Rossi<sup>2</sup>

<sup>1</sup>Visikol Inc, 675 US Highway 1, North Brunswick, NJ USA

<sup>2</sup>Corning Incorporated, Life Sciences, 2 Alfred Road,  
Kennebunk, ME USA

### Introduction

The use of three-dimensional (3D) cell cultures for *in vitro* drug discovery assays has increased dramatically in recent years because 3D cell culture models more accurately mimic the *in vivo* environment compared to traditional two-dimensional (2D) monolayer cultures. However, current imaging-based analysis of these 3D cultures relies upon techniques originally developed for 2D cell culture, and as such, has significant limitations. Specifically, the light scattering inherent with thick microscopy specimens prevents imaging the entirety of a 3D spheroid, which are typically >100 µm in diameter. This technical limitation introduces a sampling bias in imaging analysis in which only the exterior cells of a spheroid can be imaged. To accurately survey the cellular environment and response of the spheroid, the field needs new techniques to overcome the sampling bias.

Accordingly, we sought to remedy the light scattering caused by 3D spheroid opacity by employing an optical clearing agent designed specifically for spheroids, Visikol® HISTO-M™. Here, we demonstrate the utility of Visikol HISTO-M tissue clearing with HepG2 spheroids generated in Corning 96-well spheroid microplates in a high-content screening approach.

### Materials and Methods

#### Generation of Spheroids in Corning Spheroid Microplates

HepG2 cells (Sigma Cat. No. 85011430) were routinely cultured in DMEM supplemented with 10% FBS. To form spheroids, HepG2 ( $1 \times 10^3$  cells/well) were seeded into wells of 96-well spheroid microplates (Corning Cat. No. 4515) and incubated in a humidified incubator in 5% CO<sub>2</sub> at 37°C for 2 days.

#### Treatment of Spheroids with Antiproliferative Compound

A 1 mM stock solution of the antiproliferative compound paclitaxel (Alfa Aesar Cat. No. J62734MC) was prepared in DMSO. Working solutions (100X) were prepared as 10-fold serial dilutions of the DMSO stock and then diluted to final assay concentration (1 µM, 500 nM, 100 nM, 10 nM, 1 nM) in growth media. Spheroids were treated with paclitaxel on day 0 and again on day 3.

#### Fixation and Immunolabeling

On day 5, spheroids were fixed *in situ* using 10% neutral buffered formalin (NBF, Thermo Fisher Cat. No. SF100-20), followed

by washing in phosphate-buffered saline (PBS) to remove fixative. Spheroids were permeabilized with methanol, followed by 20% DMSO/methanol to improve penetration of antibodies and stains and then blocked in 10% donkey serum (Jackson Immuno Research Labs Cat. No. 017000121). Spheroids were incubated in 1:150 rabbit anti-Ki67 antibody (Thermo Fisher Cat. No. RB1510P) to label proliferating cells followed by Alexa Fluor® 488 conjugated Anti Rabbit IgG secondary (Invitrogen/Thermo Fisher Cat. No. A32731). Nuclei were stained with DAPI (Thermo Fisher Cat. No. D1306).

#### Clearing and High Throughput Imaging of Spheroids

Spheroids were cleared with Visikol HISTO-M. Briefly, this is accomplished through dehydration of the spheroids by exchange with methanol (200 µL/well for 15 min.) and subsequent exchange and transfer to the one-step immersion clearing formula, HISTO-M, for immersion clearing (200 µL/well for 30 min.). Spheroids were imaged in HISTO-M in the spheroid microplate with an IN Cell Analyzer 6000 (GE Healthcare). Z-stacks (~150 µm) were collected at 10X magnification in 5 µm steps. Images were processed using ImageJ, and DAPI+ and Ki67+ cells were counted using CellProfiler.

### Results and Discussion

#### Visikol HISTO-M Enables Visualization of Spheroid Interior

Figure 1A (top rows) feature images representative of the obstacles encountered when imaging 3D cell cultures. The interior of the spheroid appears dark, as light scattering drastically reduces fluorescence signal due to the opacity of the spheroids. Signal is only detected from the outermost cells of the spheroid. In contrast, light scattering was greatly reduced by using Visikol HISTO-M clearing agent, as evidenced by more visible nuclear fluorescence in the cleared spheroids (Figure 1A, bottom rows). This allows for comprehensive profiling of the interior of the spheroids.

#### Visikol HISTO-M Increases Detectable Cells in Interior of 3D Structure

CellProfiler was used for automated cell counting of the confocal image stacks. The data presented in Figure 1B quantifies the problems inherent with imaging non-cleared spheroids. As the image stack progresses through the non-cleared spheroid, fewer and fewer cells are detected in each plane, until only the periphery is detectable. Light scattering caused by the opacity of non-cleared

spheroids limits imaging to approximately 20 to 50  $\mu\text{m}$ , even with confocal microscopy. By clearing the spheroids, cells are detectable across the entire image plane, deep into the spheroid. On average, 3-fold more cells were detected on each plane of the cleared spheroid than the non-cleared spheroid (Figure 1B). The effect is more dramatic deeper in the spheroid; at 120  $\mu\text{m}$ , 7-fold more cells were detectable.

### Case Study: Antiproliferative Assay of HepG2 Spheroids

Control and paclitaxel-treated spheroids were imaged as above, and cell proliferation was measured as the ratio of Ki67+/DAPI+ cells to total cells (Ki67%). Dose response curves were constructed for non-cleared and cleared spheroids (Figure 2) to demonstrate the effect of spheroid resolution on proliferation assessment. Not surprisingly, there was a significant difference between the dose response curves constructed from non-cleared and cleared spheroids. The higher apparent Ki67% in non-cleared spheroids relative to cleared spheroids (Figure 2A) suggested that the outermost layer of cells, which were the only detectable cells in non-cleared spheroids, had higher levels of proliferation than the inner population. As a consequence, proliferation inhibition in non-cleared spheroids is artificially shifted towards higher paclitaxel concentrations due to the sampling bias. In fact, the Visikol HISTO-M cleared samples showed increased sensitivity in detecting inhibitory activity with significant inhibition detected at 1 nM paclitaxel compared to 100 nM required to detect signal for non-cleared control samples (Figure 2B). The  $\text{IC}_{50}$  value measured for spheroids cleared with Visikol<sup>®</sup> HISTO-M (7.01 nM) was approximately 4X lower than calculated with non-cleared control samples (29.6 nM). The increased sensitivity in cleared samples can be attributed to detection of inhibitory effects in cleared spheroids that would be obscured from detection without tissue clearing. Therefore, tissue clearing with Visikol HISTO-M eliminates the sampling bias to yield data more representative of the entire spheroid and potentially more physiological.

### Spatial Dose Response

By sampling the entire spheroid, additional downstream analysis of microenvironments within the 3D structure is made possible. Data obtained from cleared spheroids can be segregated into

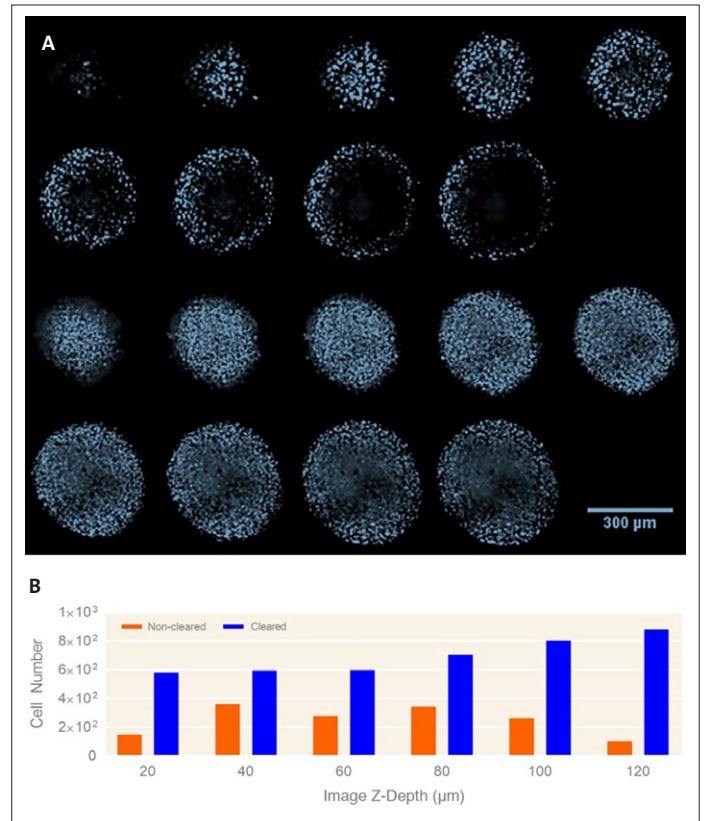


**Figure 1. Representative montage of 20  $\mu\text{m}$  slices from confocal Z-stack of DAPI-stained spheroid.** (A) Non-cleared (top rows) and cleared (bottom rows) spheroids. Scale bar = 300  $\mu\text{m}$ . (B) Number of cells detected at various Z-depth through non-cleared (orange) and cleared (blue) HepG2 spheroids.

groups based upon distance from the center of the spheroid to generate site-specific dose response curves. This allows for the investigation of potential differential response in cell proliferation due to different cellular microenvironments. In the current study, this was accomplished by calculating the center point of each of the Ki67+ nuclei detected. The center point of each spheroid was calculated as the average coordinates of the DAPI+ nuclei

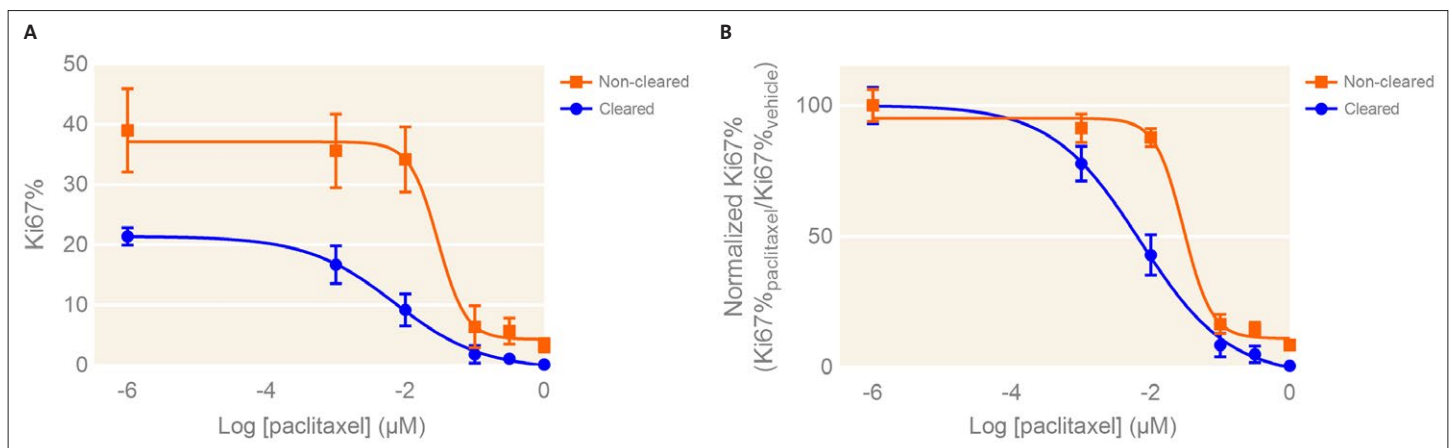


**Figure 2. Ki67% dose response curves for non-cleared (orange) and cleared (blue) HepG2 spheroids.** (A) Absolute Ki67% dose response curve for paclitaxel-treated HepG2 spheroids. (B) Normalized dose response curves showing Ki67% for paclitaxel-treated HepG2 spheroids with respect to vehicle treatment. Mean  $\pm$  SD, N = 4. \*  $p < 0.01$  via one-way ANOVA.

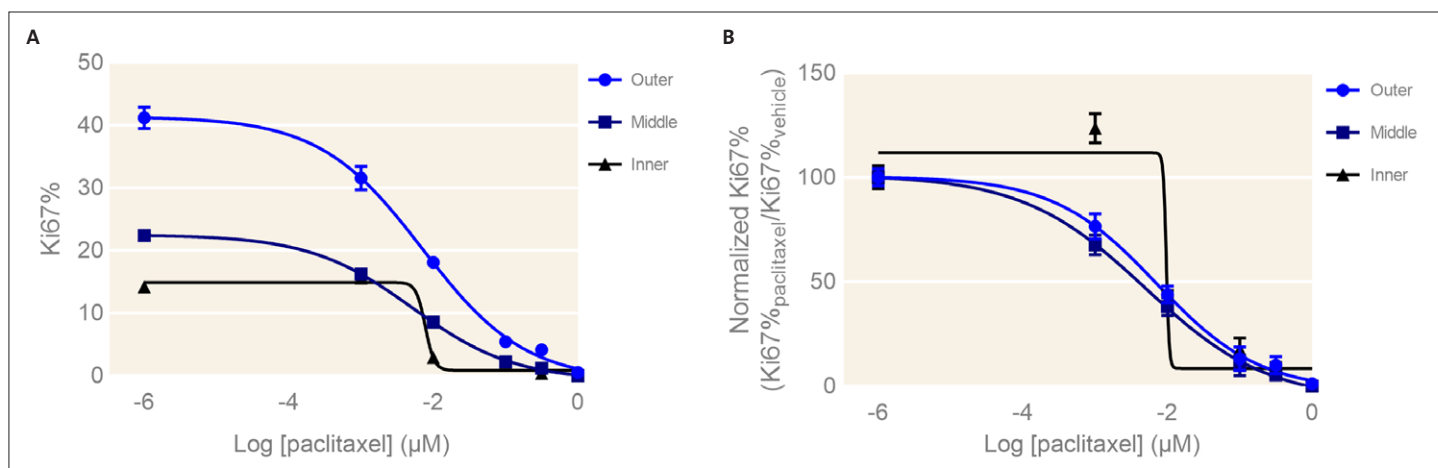


**Figure 3. Spatial dose response curves for Ki67% measured in HepG2 spheroids.** (A) Absolute Ki67% dose response curves for three populations of cells in paclitaxel-treated HepG2 spheroids. (B) Dose response curves showing Ki67% with respect to vehicle Ki67% for three populations of cells in paclitaxel-treated HepG2 spheroids. Mean  $\pm$  SD, N = 4. \* p < 0.01 via one-way ANOVA.

center points. The data were then grouped according to relative distance of each cell to the center, segregating cells into 3 concentric shells: the outer third (furthest from the center), the middle third, and inner core of cells. These data were then used to construct the spatial dose response curves shown in Figure 3.

There was a significant difference in the cell proliferation levels between the three shells of cells in vehicle and paclitaxel-treated spheroids. Consistent with the data in Figure 3, the outermost cells exhibited the highest level of cell proliferation in vehicle control (~40% cells were Ki67+). These cells demonstrated a significant sensitivity to treatment with paclitaxel, showing almost complete inhibition of cell proliferation at 100 nM paclitaxel treatment. The middle shell of cells had lower basal cell proliferation (Figure 3A), but also showed significant sensitivity to paclitaxel treatment. The innermost population of cells presented with the lowest baseline proliferation level. Interestingly, there was a significant increase in cell proliferation in the innermost population of cells with 1 nM paclitaxel treatment (Figure 3B). This is presumably due to the death of cells at the outer layers revealing new channels for nutrients and stimulating growth in otherwise quiescent cells. Nevertheless, it is clear from these results that the ability to detect differences in the effect of anti-proliferative agents in different subpopulations of cells within 3D spheroids is a valuable tool for profiling drug effects.

### Corning® Spheroid Microplates Enable Higher Throughput Imaging

Traditional flat-bottom fluorescent assay microplates suffer from two major drawbacks. First, spheroids cannot be cultured directly in the assay plate which necessitates transfer of spheroids and results in lower throughput capacity and loss of data. Second, significant time is required for the high-content imager to detect the relatively small diameter spheroids (~300  $\mu$ m) in large 5 mm diameter wells, especially at higher magnifications. This also contributes to a significant loss in assay throughput. Corning spheroid microplates allow generation and analysis of spheroids within the same plate and so, were critical to our successful high-content imaging of spheroids.

Corning spheroid microplates are black/clear-bottom microplates available in 96-well (Corning Cat. Nos. 4515 and 4520), 384-well (Corning Cat. Nos. 4516 and 3830), and 1536-well (Corning Cat. No. 4527) formats, all of which are compatible with automation systems. The Ultra-Low Attachment (ULA) surface is a hydrophilic, biologically inert, and non-degradable coating covalently attached to the interior surface of the well-bottom and promotes self-assembly of plated cells into 3D aggregates. The unique well geometry enables formation of single spheroids of uniform size across the microplate. Importantly, spheroids tend to settle in the bottom of the unique U-shaped wells which simplifies and accelerates the imaging process, as less time is required to scan the well to find the spheroid. The opaque side walls and proprietary gridded plate bottom design reduce well-to-well cross-talk and background fluorescence/luminescence. Ultimately, the novel and

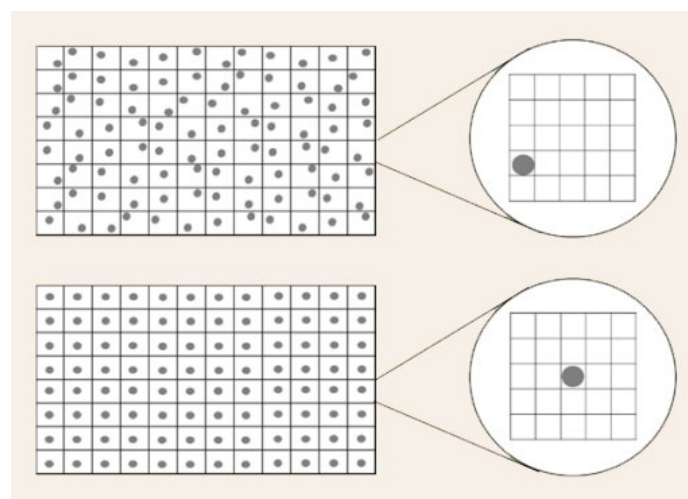


**Figure 4. Spheroid positioning in conventional flat-bottom microplates vs. Corning spheroid microplates.** Conventional flat-bottom 96-well microplates result in randomly positioned spheroids, thus a much larger area must be scanned by the high-content imager to find the spheroid to image, reducing throughput. Corning 96-well spheroid microplates, with their unique U-shaped well bottom, center the spheroids permitting accelerated image acquisition.

proprietary design of the spheroid microplates positions them as an ideal tool for high throughput analysis of 3D cell cultures.

Furthermore, the Corning® spheroid microplates are chemically compatible with Visikol® HISTO-M clearing. The Visikol clearing process, which takes only minutes, can be done within the spheroid microplate wells. The present study demonstrates the advantages of tissue clearing in imaging analysis of spheroid cultures. Namely, clearing of spheroids allows for query of the entirety of the 3D structure and, thus, a more thorough analysis of the microenvironments within the spheroid. In short, uniform spheroids can be reproducibly generated and cultured, labeled, cleared, and imaged in Corning spheroid microplates without the transfer of spheroids, ensuring a comprehensive data set without the loss of information or throughput.

### Advantages of Corning Spheroid Microplates for High-content Imaging

- ▶ Visikol HISTO-M is compatible with immunolabeling and fluorescent staining of spheroids
- ▶ Novel well geometry aids centering of spheroid position for automated high-content imaging
- ▶ Single field of view
- ▶ Standard 96-, 384-, and 1536-well spheroid microplate dimensions allow robotic automation
- ▶ Microplates amenable to confocal high-content imaging
- ▶ Opaque black side-walls minimize well-to-well fluorescent cross-talk
- ▶ Flexibility of antibodies and dyes
- ▶ Single plate assay (i.e., culture and assay of spheroids in the same microplate) allows for easier high throughput production and handling of spheroids

For more specific information on claims, visit the Certificates page at [www.corning.com/lifesciences](http://www.corning.com/lifesciences).

**Warranty/Disclaimer:** Unless otherwise specified, all products are for research use only. Not intended for use in diagnostic or therapeutic procedures. Corning Life Sciences makes no claims regarding the performance of these products for clinical or diagnostic applications.

### Conclusions

- ▶ Visikol HISTO-M is compatible with immunolabeling and fluorescent staining of spheroids.
- ▶ Clearing spheroids with Visikol HISTO-M enables visualization of the interior of spheroids.
- ▶ Cleared spheroids deliver >3X higher cell counts in high-content confocal image analysis.
- ▶ Data obtained from Visikol HISTO-M represents the whole of the spheroid because interior cells are detectable.
- ▶ The novel well geometry of Corning spheroid microplates enables high quality automated imaging of spheroids for high-content screening approaches, allowing multiplexed cell health analysis to be performed *in vitro* with physiologically relevant 3D models.

For more information about Visikol HISTO-M, visit [visikol.com/visikol-histo-m/](http://visikol.com/visikol-histo-m/)

For additional product or technical information, visit [www.corning.com/lifesciences](http://www.corning.com/lifesciences) or call 800.492.1110. Outside the United States, call +1.978.442.2200 or contact your local Corning sales office.

# CORNING

**Corning Incorporated**  
*Life Sciences*

836 North St.  
Building 300, Suite 3401  
Tewksbury, MA 01876  
t 800.492.1110  
t 978.442.2200  
f 978.442.2476

[www.corning.com/lifesciences](http://www.corning.com/lifesciences)

#### ASIA/PACIFIC

**Australia/New Zealand**  
t 61 427286832

**China**  
t 86 21 3338 4338  
f 86 21 3338 4300

**India**  
t 91 124 4604000  
f 91 124 4604099

#### Japan

t 81 3-3586 1996  
f 81 3-3586 1291

#### Korea

t 82 2-796-9500  
f 82 2-796-9300

#### Singapore

t 65 6572-9740  
f 65 6861-2913

#### Taiwan

t 886 2-2716-0338  
f 886 2-2516-7500

#### EUROPE

CEurope@corning.com

#### France

t 0800 916 882  
f 0800 918 636

#### Germany

t 0800 101 1153  
f 0800 101 2427

#### The Netherlands

t 020 655 79 28  
f 020 659 76 73

#### United Kingdom

t 0800 376 8660  
f 0800 279 1117

#### All Other European Countries

t +31 (0) 206 59 60 51  
f +31 (0) 206 59 76 73

#### LATIN AMERICA

grupoLA@corning.com

#### Brasil

t 55 (11) 3089-7400

#### Mexico

t (52-81) 8158-8400